biomass

MDPI

Article

Construction of an Automated Biochemical Potential Methane (BMP) Prototype Based on Low-Cost Embedded Systems

Sergio Arango-Osorio, Carlos Alejandro Zuluaga-Toro, Idi Amín Isaac-Millán, Antonio Arango-Castaño and Oscar Vasco-Echeverri [1,*]

Transmission and Distribution of Energy T&D Group, Universidad Pontificia Bolivariana, Medellín 050001, Colombia; searango@ttu.edu (S.A.-O.); carlos.zuluaga@upb.edu.co (C.A.Z.-T.); idi.isaac@upb.edu.co (I.A.I.-M.); antonio.arango@upb.edu.co (A.A.-C.)

* Correspondence: oscar.vasco@upb.edu.co; Tel.: +57-(604)-448-8388 (ext. 12175)

Abstract

Anaerobic digestion is a sustainable approach for waste treatment and renewable biogas production. A key parameter for large-scale applications is the Biochemical Methane Potential (BMP), which enables methane yield estimation and facilitates process scale-up. This study introduces an automated, low-cost prototype for BMP testing, comprising three 2-L reactors with provisions for future expansion. Control and data acquisition are carried out by low-cost embedded systems integrated with sensors for pressure, temperature, pH, and biogas flow. The system was evaluated using a mixture of pig manure and sludge from a local wastewater treatment plant. Real-time monitoring of temperature, pH, and biogas production was achieved. The heat exchanger, designed through transient energy balance modeling, increased the reactor temperature from 20 °C (lab temp.) to 38 °C in 400 s. Overall, the prototype demonstrated reliable performance, achieving rapid heating, stable monitoring, and precise biogas flow quantification through both displacement and pressure methods.

Keywords: anaerobic digestion; biochemical methane potential (BMP) ; renewable energy; automated prototype; sensor-based acquisition

check for updates

Academic Editor: Borja Velazquez-Marti

Received: 26 August 2025
Revised: 23 September 2025
Accepted: 26 September 2025
Published: 3 November 2025

Citation: Arango-Osorio, S.; Zuluaga-Toro, C.A.; Isaac-Millán, I.A.; Arango-Castaño, A.; Vasco-Echeverri, O. Construction of an Automated Biochemical Potential Methane (BMP) Prototype Based on Low-Cost Embedded Systems. *Biomass* **2025**, *5*, 68. https://doi.org/10.3390/biomass5040068

Copyright: © 2025 by the authors. Licensee MDPI, Basel, Switzerland. This article is an open access article distributed under the terms and conditions of the Creative Commons Attribution (CC BY) license (https://creativecommons.org/licenses/by/4.0/).

1. Introduction

Anaerobic digestion (AD) is a sustainable and efficient technology for treating organic waste. It produces biogas, a renewable energy source that can substitute fossil fuels, mitigate greenhouse gas emissions, reduce deforestation, and generate high-quality fertilizer, particularly in developing countries [1,2]. This by-product, is rich in nutrients such as nitrogen and phosphorus, making it suitable for agricultural applications [3,4]. Globally, large amounts of organic waste are generated, which can be converted into both biogas and organic fertilizer through AD technology [5]. This represents a major opportunity to enhance quality of life while contributing to the bioeconomy, public health, and environmental sustainability worldwide [6].

AD can process a wide variety of organic wastes using different types of bioreactors [7]. To optimize the reactor design and operation, the Biochemical Methane Potential (BMP) test is employed to determine the methane yield of specific substrates [8]. BMP tests are widely recognized as the state-of-the-art method for assessing methane yield and are therefore essential for the design and scaling of anaerobic digesters [9]. In recent years,

interest in BMP testing has increased significantly, as evidenced by the growing number of publications on this topic [10].

BMP tests are valuable tools for both researchers and practitioners. They have been applied to identify suitable feedstocks for AD [11], to evaluate the ultimate methane yield of substrates used in modeling approaches [12], and to provide critical information for determining organic loading rates and hydraulic retention times [13].

However, comparing BMP results across studies remains challenging due to differences in methodologies, operating conditions, equipment, and pretreatment procedures [14–16]. Several standardized BMP protocols have been developed, including the method proposed by Angelidaki et al. in 2009 [8], the 2011 VDLUFA guidelines [17]. In 2015, an international initiative was launched to improve reproducibility in BMP testing, leading to new guidelines and validation criteria [18,19], thereby strengthening the reliability of results, enhancing cross-laboratory comparability, and fostering global standardization in anaerobic digestion research. The VDI 4630 protocol published in 2016 [20] is extensively applied in Germany, where more than 30 laboratories routinely use it for BMP characterization, establishing it as the benchmark method in anaerobic digestion research. Its application has also been consolidated in other European countries, including the Technical University of Denmark, Lund University in Sweden and both BOKU–University of Natural Resources and Life Sciences and the University of Innsbruck in Austria. Beyond Europe, institutions such as the Institute of Environment, Natural Resources and Biodiversity (IRENA) at Universidad de León (UL) in Spain and the Universidad Pontificia Bolivariana (UPB) in Colombia have likewise adopted this protocol.

Table 1 offers a detailed overview of the main points and limitations of various Biochemical Methane Potential (BMP) methods, compared with the BMP analysis recommended in the referenced study. It highlights the strengths and weaknesses of each approach, including factors such as reproducibility, substrate specificity, operational complexity, and potential sources of error. By presenting this comparison, the table aims to provide readers with a clearer understanding of how alternative methods measure up against the standard BMP protocol, helping to inform method selection and experimental design.

This study presents the design and construction of an automated BMP measurement prototype developed at Universidad Pontificia Bolivariana (UPB) in Colombia, which integrates a Programmable Logic Controller (PLC) to enable real-time monitoring, control, and data acquisition. The system integrates bioreactors with temperature control, biogas volume quantification, and a data acquisition platform based on low-cost embedded systems. The prototype was tested with pig manure and sludge from a wastewater treatment plant, enabling real-time monitoring of pH, temperature, and methane production.

The system offers several advantages over traditional methodologies used to determine BMP. Being an automated, low-cost prototype, it facilitates the measurement process and reduces the need for manual labor compared to protocols such as the VDI 4630 standard, which are typically more expensive and complex. The incorporation of pressure, temperature, pH and biogas flow sensors also allows for real-time monitoring of digestion conditions, representing a significant advance over the classic Owen et al. method and responding to Angelidaki and Holliger's recommendations regarding the control of critical variables. Furthermore, the built-in heat exchanger allows for rapid and stable achievement of mesophilic conditions, reinforcing the system's reliability.

Still, the prototype has some clear limits. Unlike well-established protocols, it has not been tested across different laboratories, which means its results cannot yet be compared with confidence. Its small scale, using only three two-liter reactors, also weakens the strength of the tests and makes the data less representative. In addition, because it is not

officially recognized as a standard, unlike VDI 4630, it carries no regulatory weight. Also, the system does not include some key methodological steps described in the guidelines of Angelidaki and Holliger, such as setting the right inoculum-to-substrate ratio, adding proper controls, and defining clear criteria for when the tests should end.

Table 1. Principal BMP methods found.

Method	Main Elements	Limitations
Classical batch test [21]	It was a foundational method for BMP analysis. It is simple and low cost, uses sealed reactors and allows measurement of both total biogas and its methane content	It shows high variability, lacks standardized control criteria and is therefore difficult to compare across laboratories
Angelidaki et al. control reactor [8]	It can be considered the basis for international harmonization of the BMP protocol. Applicable to both solid and liquid wastes, includes a defined inoculum-to-substrate ratio, blanks and positive controls, mesophilic incubation, mixing and standardized gas measurement	It is not an official standard and has therefore been only partially adopted by laboratories
VDI 4630 [20]	A recognized and reproducible standard, widely applied in Europe. Its rigorous technical framework, defines reactor volume, number of replicates, temperature, termination criteria, blanks and control	Complex technical approach, paid document, and less accessible outside Germany
Holliger et al. [18]	International consensus document that provides inter-laboratory quality improvement. It includes mandatory controls, standardization for volatile solids, correction for inoculum production and stabilization criteria	It is not intended to replace or rewrite the standard. It is used as a guide and not as a legal standard

2. Materials and Methods

The automated BMP prototype Figure 1a consists of three batch reactors with identical geometry, selected to ensure statistical validity and reproducibility [22]. The system is scalable in multiples of three, allowing for simultaneous testing. Each reactor includes a jacketed heat exchanger supplied with recirculating hot water, as well as temperature, pressure and pH sensors. Biogas production is estimated indirectly using the ideal gas law and a custom-built flow meter developed in this study. Stirring mechanisms were excluded, as the prototype is designed for diluted or easily degradable substrates, where mixing is not required, as supported by one of the studies consulted [23].

Figure 1b shows the general dimensions of the prototype, which was designed for easy mobility. The system allows for scalability, enabling the addition of more reactors (up to 15) either on the same or a second level, depending on space availability. The heat exchanger system was also designed with this expansion in mind. The general BMP process is detailed in the PID diagram (Figure 2), which outlines the components, the process flow and the electronic devices involved in the temperature, pressure control and data acquisition. The acronyms R1, R2 and R3 correspond to the three reactors; LS and TS denote the level switch and the temperature switch, respectively; TK1 identifies Tank 1 and P1 refers to Pump 1. The terms used in the equations represent the readings from the temperature and level transmitters, while the others are only intended to identify the system components.

The heating system uses galvanized steel pipes (¼ inch or 6.35 mm diameter) to circulate hot water, shown as continuous lines in the diagram. The system allows the

connection of up to 12 additional reactors via valve SV-4. Its design was based on the heat exchanger capacity and pump power to ensure efficient thermal performance.

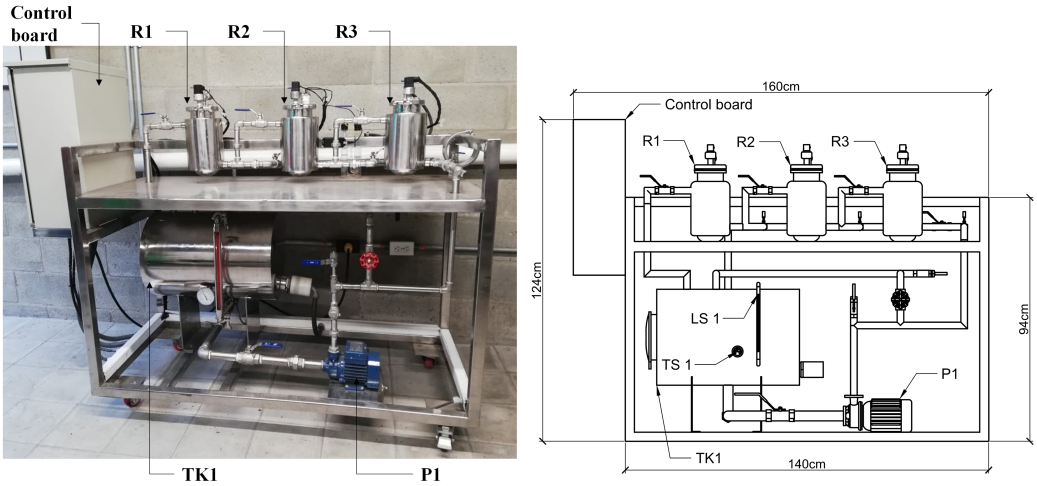


Figure 1. (**a**) Automated BMP Prototype for diluted feedstock. (**b**) Prototype Diagram in the first-step design.

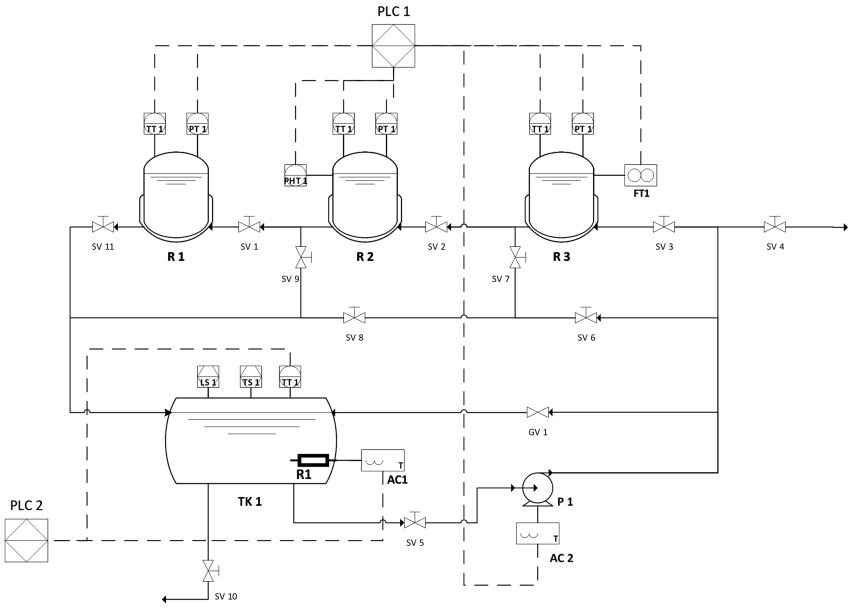


Figure 2. Process and Instrumentation Diagram (P&ID) of the BMP prototype.

2.1. Heat Exchanger Configuration

Maintaining a constant temperature is essential in the BMP system to ensure reproducible results. The heating system uses recirculating hot water circulated through jacketed reactors, heated by an electric resistance inside a 50-L tank (Figure 3). A centrifugal pump [24] drives the water through the system: from the tank to the reactor jackets and then back to the tank in a closed loop.

The heating system uses a centrifugal pump, designed based on pipe length and a minimum flow rate of 40 L/min. This ensures rapid heat transfer, allowing a quick temperature increase in the reactors and anticipating the thermal demand of future reactor expansions. The hot water circulates through a network of connected pipes and fittings, directing flow through the reactor jackets. The pump design was based on mass conservation principles

for incompressible fluids in steady state, and its maximum head was estimated using the following expression (1) [24]:

$$h_{(pump,\mu)} = (z_1 - z_2) + h_L \tag{1}$$

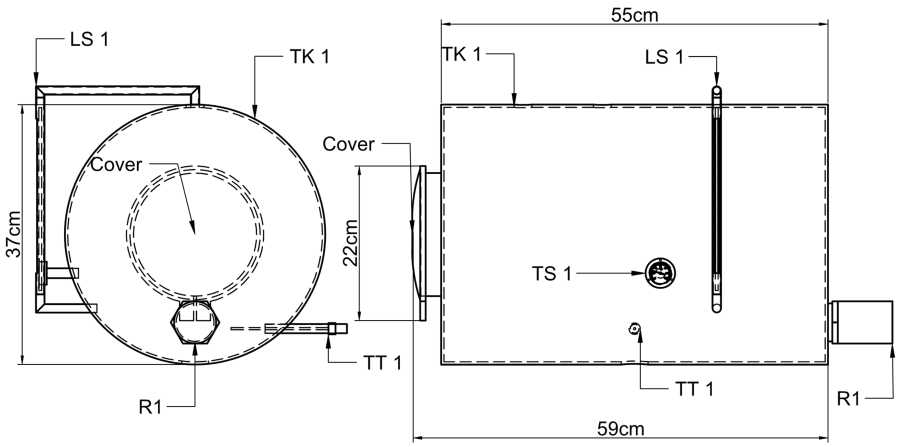


Figure 3. Frontal and lateral Views of the Heated Tank (TK 1).

Since the system operates in recirculation, the elevation difference between the supply and return points is assumed to be zero, making the elevation term equal to 0. Therefore, the maximum pump head was estimated using (2):

$$h_{(pump,\mu)} = h_L = (f \cdot \frac{L}{D} + \sum K_L) \cdot \frac{V^2}{2g} \tag{2}$$

Which explains that pressure losses in the piping system are caused by friction and fittings. The friction factor is determined using the average velocity (3), the Reynolds number (4), and the Colebrook Equation (5), as detailed below.

$$v = \frac{Q}{\Pi \cdot \frac{D_i^2}{4}} \tag{3}$$

$$R = \frac{\rho \cdot v \cdot D_i}{\mu} \tag{4}$$

$$\frac{1}{\sqrt{f}} = -2.0log(\frac{\epsilon}{3.7 \cdot D_i} + \frac{2.51}{Re \cdot \sqrt{f}}) \tag{5}$$

Head losses from fittings and accessories were estimated using loss coefficients proposed by Çengel and Cimbala [24]. The list of accessories and their corresponding loss coefficients is presented in Table 2.

Table 2. Inventory of pipes accessories and losses coefficients.

Accesory	Loss Coefficient	Quantity	$\sum K_L$
90° Elbow standard	1.1	9	9.9
Ball valve open	0.05	4	0.2
Reactor jackets	1	3	3
90° T connectors	2	3	6

The pump power was calculated using Equation (6). The system of equations was solved in MS Excel using an iterative numerical method (affine homotopy).

$$W_{(pump)} = \frac{\rho \cdot Q \cdot g \cdot h_{(pump,\mu)}}{\eta_{(engine-pump)}} \quad (6)$$

2.2. Reactor Design Parameters

The reactor design started with defining the volume and number of units. The volume was selected based on heuristic guidelines proposed by experts in anaerobic digestion [23], while the number of reactors (replicates) was determined following statistical principles for data analysis and reproducibility [22]. The dimensions of the reactor, diameter and height, were calculated using Equations (7) and (8) [6].

$$D_R = \sqrt[3]{\frac{4 \cdot V}{\pi \cdot (\frac{L}{D})_R \cdot (1 - Vf_R)}} \quad (7)$$

$$L_R = (\frac{L}{D})_R \cdot D_R \quad (8)$$

The reactor diameter was chosen based on the availability of stainless steel SCH 40 pipes in the local market. The height was determined using the length-to-diameter ratio $(L/D)_R$, and the reactor volume—ranging from 125 mL to 2000 mL was estimated using Equations (7) and (8) [25]. The selected heat exchange system was jacketed heating, suitable for small reactors, requiring low operating temperatures and lower capital costs (CAPEX) compared to other systems. The energy balance for the jacket design is shown in Equation (9) [26].

$$\frac{dT_i}{dt} = \frac{W \cdot Cp_C}{M \cdot Cp_H} \cdot (\frac{K-1}{K}) \cdot (T_H - T_i) \quad (9)$$

where K is calculated according to Equation (10).

$$K = e^{\frac{U \cdot A}{W \cdot Cp_C}} \quad (10)$$

Based on the recommended hot water outlet temperature, a global heat transfer coefficient of 0.5 was used [27]. The thermal system was simulated using Polymath® software, applying the Runge-Kutta 45 (RKF45) numerical method.

2.3. Control System and Data Acquisition

The control and data acquisition system consists of two control loops, as shown in Figure 4. The first loop, managed by PLC1 (Arduino Mega2560 and Raspberry Pi 3, Somerville, MA, USA), controls the on/off state of the recirculation pump to maintain the internal reactor temperature at the selected set-point. It also receives analog and digital signals from the pressure sensor (Wika/Eco-1, Klingenberg am Main, Germany), pH sensor (Dfrobot/Sen0161, Shanghai, China), and a homemade flow sensor developed at UPB-UL.

The second loop, operated by PLC2 (Autonics TK4 series), manages the heating system. This loop maintains a higher set-point than the reactor's internal temperature and regulates a 300 W electric heating resistance using an RTD Pt100 temperature sensor. The temperature sensor used in the system is a Dallas/DS18B20 by Analog Devices (known befores as Maxim Integrated/Dallas Semiconductor), in Wilmington, MA, USA, and the heating circuit is controlled through contactors ABB/A110-30-11 (AC1) and LC1/D09 1G (AC2). The complete power and logic wiring diagram is shown in Figure 4, accompanied by a nomenclature table describing the referenced components.

Figure 4 illustrates the configuration of the control and power system. At the top, the connection of the pump motor along with its respective protective devices is presented. On the right-hand side, the single-line diagram of the alternating current supply system

is shown, together with the corresponding AC–DC converters. In the central section, the high-level control unit implemented through a Raspberry Pi board is displayed on the left, while on the right, the data acquisition system managed by an Arduino ATMEGA board is depicted. At the bottom, the connection of the pH meter is indicated. Surrounding the data acquisition system, the figure also details each of the sensors integrated into the system. The colors on the lines are only to visually differentiate the connections.

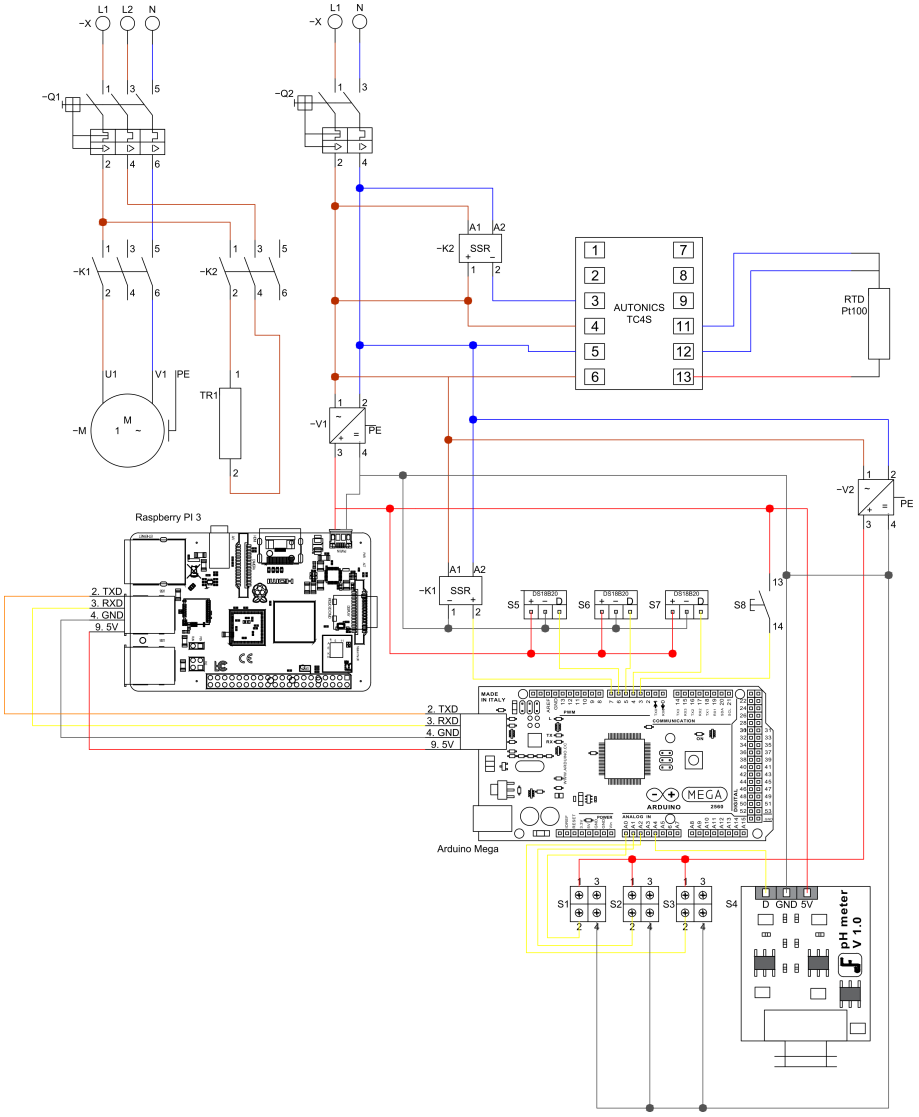


Figure 4. Power and logic line diagram to electrical connection in the BMP test prototype.

2.3.1. Temperature Sensors Connection to PLC1

The digital temperature sensors (Dallas, DS18B20) are connected to the Arduino Mega 2560 via digital ports 4, 5, and 6, assigned to reactors 1, 2, and 3 respectively, as shown in Figure 5. These sensors transmit data in binary format, which is converted to decimal using the corresponding sensor library [28,29]. The sampling interval is set to 1 s, with the program outputting the average temperature every 30 min. As in the previous diagram, the color of the lines is not intended to distinguish any particular element.

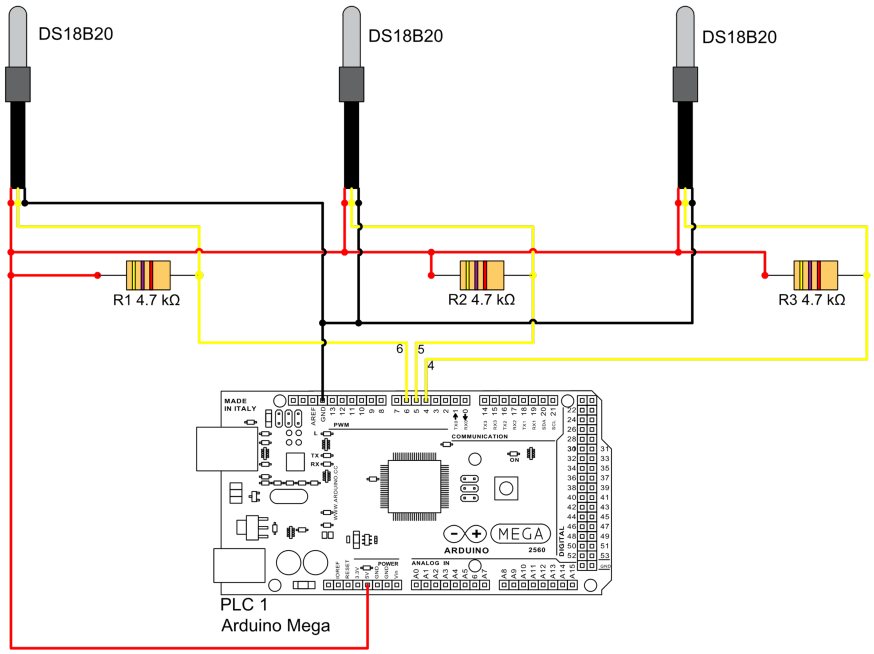


Figure 5. Power and logic line diagram of electrical connection in the Arduino Mega.

2.3.2. Pressure Sensors Connection to PLC1

The pressure sensors (Wika Eco-1), which measure a range of 0–15 psig, transmit a 4–20 mA analog signal and require a 24 VDC power supply. They are connected to PLC1 through analog ports A0, A1 and A2 (Figure 6). To convert the signal to 0–5 VDC, 220 Ω resistors were used. The ground terminals of the 24 VDC and 5 VDC power sources are unified to prevent sensor or equipment malfunction. The color of the connection lines does not differentiate any element.

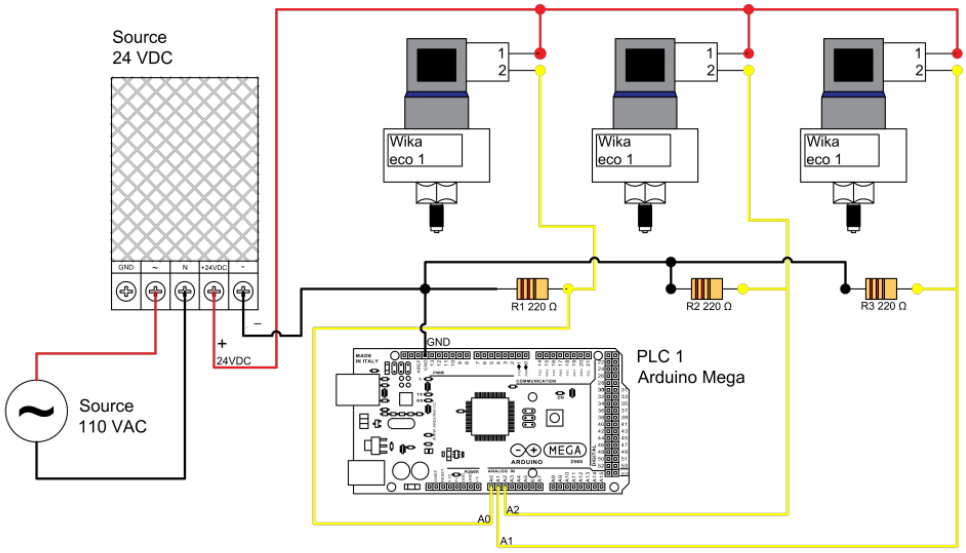


Figure 6. Power and logic line diagram of electrical connection between the Arduino Mega, the source of power and the pressure sensors.

An analog manometer (Test Gauge, PGS-35L-30, Palmetto, FL, USA) was used to calibrate the pressure sensors. Equation (11) was applied for the 0–3 psig range, while Equation (12) was used for measurements between 3–15 psig. Based on prior experi-

ence with similar calibration approaches, this method provides a reliable way to validate sensor performance.

$$P = \frac{4653 \cdot V_1 + 0.0405 \cdot (V_1 - 175)^3 - 814,206}{1,000,000} \quad (11)$$

$$P = 0.02553 \cdot V_1 - 9.9647 \quad (12)$$

2.3.3. pH Sensor Connection to PLC1

For pressures below 3 psig, a polynomial linear regression was used to obtain the calibration curve, while for pressures above 3 psig, a simple linear regression was applied [30]. The pH sensor (DFRobot®, SEN0161) emits a 0–5 VDC analog signal and is connected to analog port A4 of the Arduino. It is powered by a 5 VDC supply from the Arduino itself (Figure 7). The color of the connection lines does not differentiate any element.

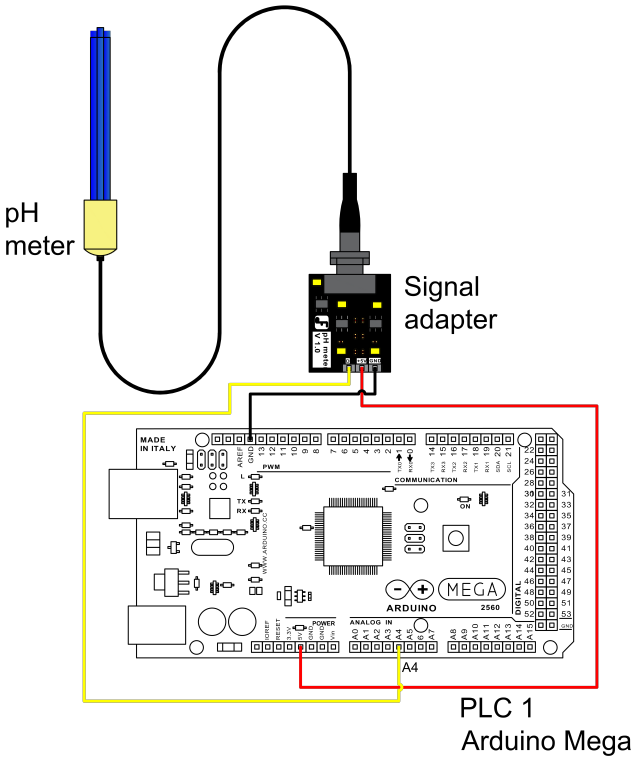


Figure 7. Schematic diagram for the connection between the PH-meter and AM2560.

The calibration curve for the pH sensor was developed using Equation (13), as recommended by the manufacturer [31].

$$pH = (\frac{V_1 \cdot 5}{1023}) \cdot 3.5 \quad (13)$$

2.4. Control System Using the PLC1 for the Pump Operation

The On/Off pump control, managed by PLC1 (Figure 8), regulates the internal reactor temperature. BMP tests are typically performed under mesophilic conditions (35 ± 2 °C) [32], but the prototype also supports operation at 55 °C and could be adapted for psychrophilic conditions with minor modifications. The colors of the connections are not meant to indicate any difference.

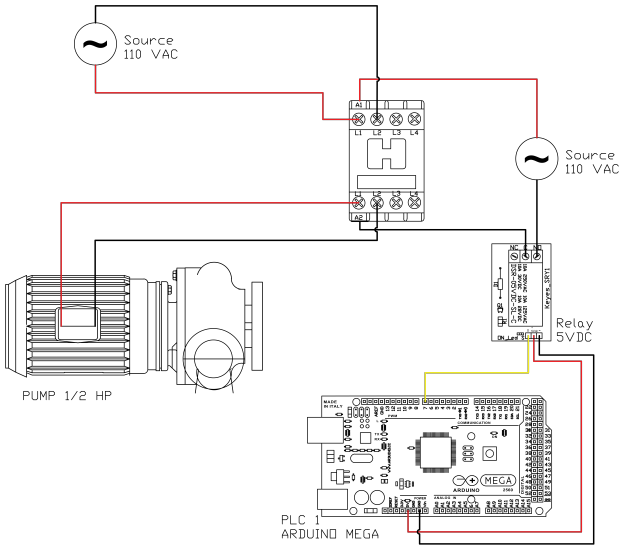


Figure 8. Schematic diagram of On/Off control connection for the pump to recirculate hot water through the jacket-exchanger system.

2.5. Flow Sensor for the Biogas Produced

Technological surveillance was conducted to develop a flow meter suitable for low biogas production (0.01–1 L/min). Koch et al. reported less than 5 % difference between manometric and gravimetric methods [33]. In this study, a siphon-based displacement flow meter designed by the IRENA group at the Universidad de León was used (Figure 9).

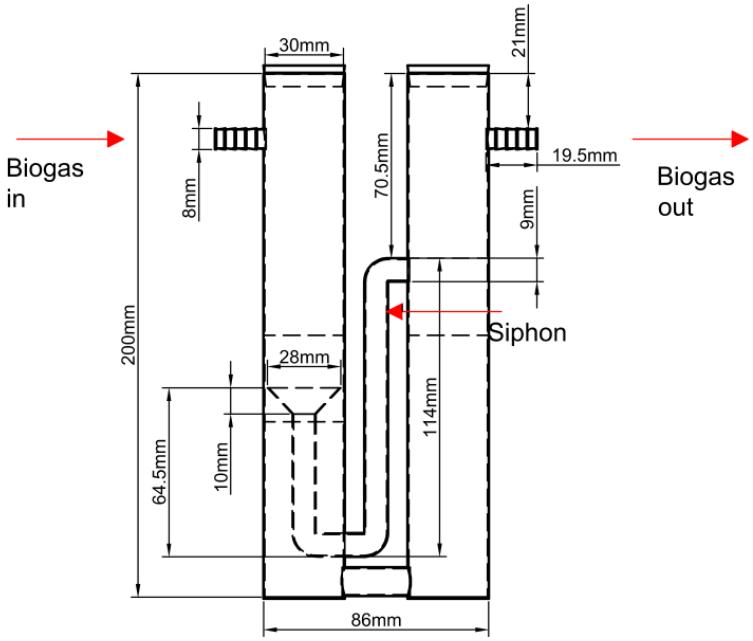


Figure 9. Schematic diagram of the flow sensor used in the prototype.

The flow meter operates by detecting pressure increases in the left compartment due to biogas production from the reactor. This pressure displaces water through a siphon into the right compartment. When the water in the right compartment reaches a maximum level, an electronic circuit registers a count, after which the water returns to the left compartment and the cycle repeats. The count signal is sent to PLC1 (Figure 10), where it is processed and stored. The colors of the connections are not meant to indicate any difference.

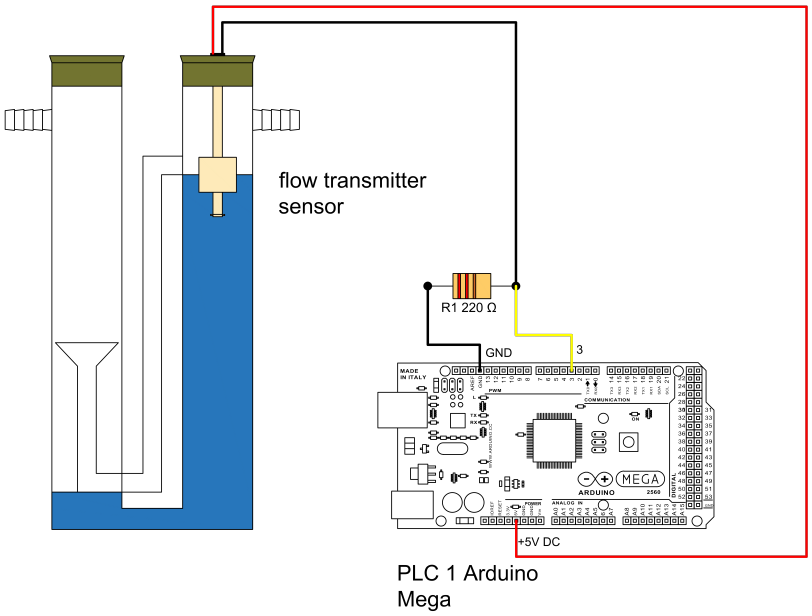


Figure 10. Diagram for the connection of Gas-flow sensor to AM2560.

Daily samples were collected from the headspace of the reactors and analysed by gas chromatography (GC) using a GC Agilent 6890A from Agilent Technologies, in Santa Clara, CA, USA, which was equipped with HP-PLOT/Q and HP-MOLSIEVE columns, in order to determine the concentrations of methane, carbon dioxide and other trace gases [25].

2.6. PLC2 Connection to Control the Temperature in the TALT

Temperature control was achieved using an Autonics TC4S temperature controller, an RTD pt100 sensor (as mentioned before, it is a Dallas/DS18B20 by Analog Devices (formerly Maxim Integrated/Dallas Semiconductor), based in Wilmington, MA, USA) and a 1.5 kW electric resistance. The ABB AF30-0013 contactor, activated by a universal relay ABB CR-U230AC2, controls the resistance. As shown in Figure 11, the electric resistance is triggered by the controller's ignition coil through pins 3 and 4, maintaining a stable temperature according to the selected temperature control set-point. All connections serve the same purpose, regardless of their color in the diagram.

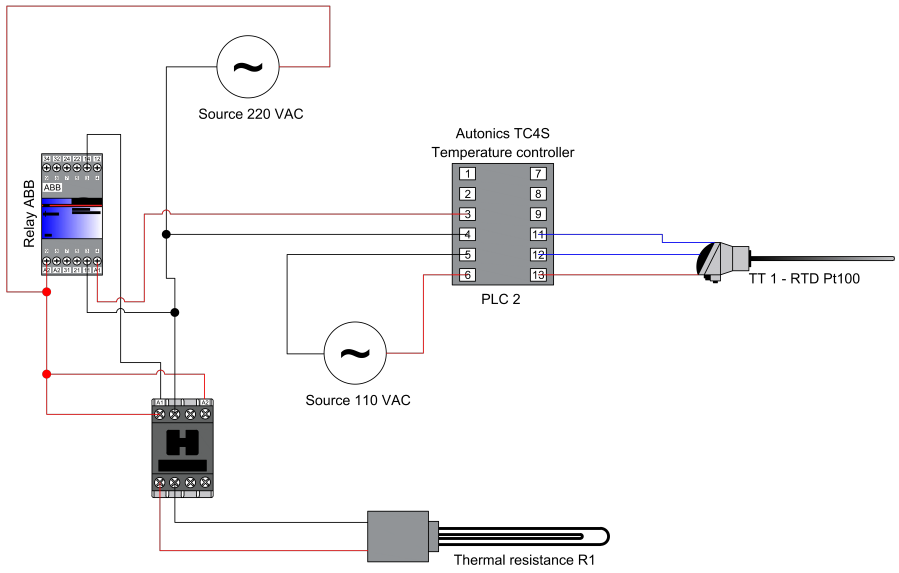


Figure 11. Diagram for the connection of temperature control.

2.7. PLC1 Configuration

PLC1 consists of an Arduino Mega 2560® (AM2560) and a Raspberry Pi 3 Model B® (RBP3), which includes additional USB and Ethernet ports [34]. The two devices are connected via a USB cable, as shown in Figure 12. The Arduino is powered through this cable with 5 VDC supplied by the Raspberry Pi, which also enables data communication. A serial protocol at 9600 bps was configured, using four lines: pin 2 for transmitted data (TXD), pin 3 for received data (RXD), pin 4 for ground and pin 9 for voltage. The Arduino was configured using the free Integrated Development Environment (IDE) available on the Arduino website [35] and programmed using an object-oriented programming language.

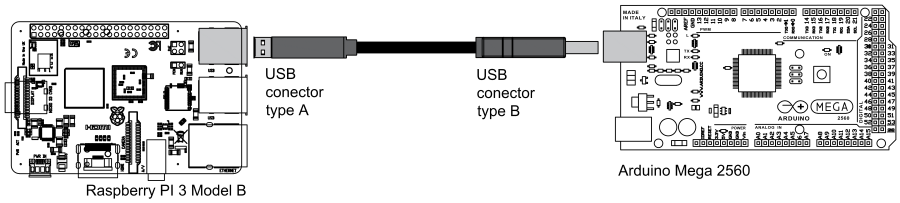


Figure 12. Diagram for the connection of Arduino Mega 2560® and Raspberry Pi 3 Model.

2.8. Raspberry PI 3® Configuration to Data Storage

The Raspberry Pi 3® was used to capture and store data from the Arduino Mega® due to its easy integration, simple programming, versatile communication protocols, low cost and local availability. It was configured using the Raspbian® operating system and the open-source software Node-RED® by IBM®, which enables a block-based interface for data acquisition and storage, as shown in Figure 13. The numbers are intended to guide the sequence of steps for data management.

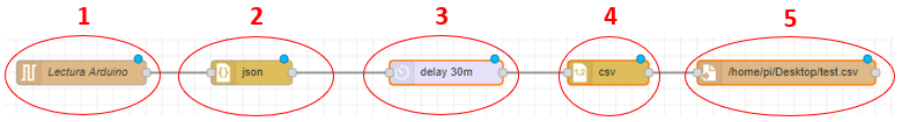


Figure 13. Node-RED code for data management using Arduino Mega®.

In the Node-RED® configuration: Node 1 establishes unidirectional communication between the Arduino Mega® and Raspberry Pi 3® via a 9600 baud serial port in STRING format; Node 2 converts the data from STRING to JSON; Node 3 introduces a 30-min delay to store one data point every 30 min; Node 4 converts the JSON to CSV format; and Node 5 assigns a local path for data storage.

2.9. Function Test, Manure Pig BMP Test

Once the prototype was built, a BMP test was conducted using pig manure as substrate and sludge from the San Fernando WWTP in Medellín-Colombia as inoculum. Both were characterized beforehand by analyzing Total Solids (TS) and Volatile Solids (VS) according to APHA standards [36]. The substrate-inoculum mixture was prepared using a 2:1 VS ratio [37], measured with an analytical balance, and adjusted with water to the final volume before being fed into the sealed reactors. Based on these values, the mixture was prepared with 178 g of pig manure, 107 g of WWTP sludge and 1.215 g of water to fill 90% of the reactor volume. Throughout the test, pH, temperature, flow and pressure were continuously monitored. The equipment was then activated for control and data acquisition. The test lasted 22 days at a set temperature of 37 °C. Every four days, methane concentration in the headspace gas was measured using a calibrated IMR 2800P biogas analyzer. Additionally, pH was adjusted using 1 M NaOH and monitored every 30 min. The results are presented below.

3. Results

After completing the construction and calibration of the prototype, a BMP test was conducted using pig manure as substrate and sludge from a municipal wastewater treatment plant as inoculum. The system operated under controlled mesophilic conditions (37 °C) for 22 days, during which data on biogas production, methane concentration, and pH stability were collected. The following section presents and analyzes the results obtained from this experimental run.

3.1. Selection of the Pump in the Heat Exchanger Configuration System

The pump for the prototype was selected based on the power required to recirculate the thermal fluid through the three reactor jackets. This power was calculated by solving the equation system described previously, assuming a steady-state, incompressible and turbulent flow. Inflow effects were considered negligible, and a flow rate of 40 L/min was assumed, using the average properties of water at 37 °C (see Table 3).

Table 3. Results of the pump system design.

Water Properties and Operation Conditions		**Pipe Parameters**	
ρ (kg/m^3)	994	D_i (m)	1.58×10^{-2}
μ (kg/m·s)	6.53×10^{-4}	ε (m)	4.50×10^{-5}
$\dot{v}$ (m^3/s)	6.67×10^{-4}	L (m)	3.24
$\eta_{\text{engine–pump}}$	0.3		
Calculated parameters			
h_{pump}, μ (m)	14.57	v (m/s)	3.40
Re	8.18×10^4	f	2.74×10^{-2}
W_{pump} (W)		315.73	

According to the design, a 0.5 hp centrifugal pump (Pedrollo, PKM60) was selected, and a globe valve was installed upstream to regulate the recirculation flow. The pipe and pump system allows the future addition of new reactors. Although this would increase the pump load, the overall efficiency is expected to improve, as indicated by the pump's characteristic curves [38].

3.2. Results of Reactor Design

The reactor was sized considering its total volume, free volume fraction, and height-to-diameter ratio. The diameter and height were calculated using Equations (7) and (8), respectively. The sizing results are presented in Table 4.

Table 4. Dimensions of the designed reactors.

Parameter	**Notation**	**Value**	**Units**
Reactor volume	V	1.9	Litre
Free-volume fraction of the reactor	V_{fR}	15	%
Height-diameter ratio	$\left(\frac{L}{D}\right)_R$	2.5	– (ad.)
Internal reactor diameter	D_R	9.9	cm
Reactor height	L_R	25	cm

A volume of 2000 mL was selected, as it is more suitable for heterogeneous substrates. Although smaller bottles are sometimes used, Pearse et al. argue that they may not reflect realistic operating conditions due to smaller microbial consortia and lower VFA concentrations compared to larger-scale reactors [39]. Based on the results in Table 4, the reactor was designed using AutoCAD 2019®, with dimensions detailed in Figure 14.

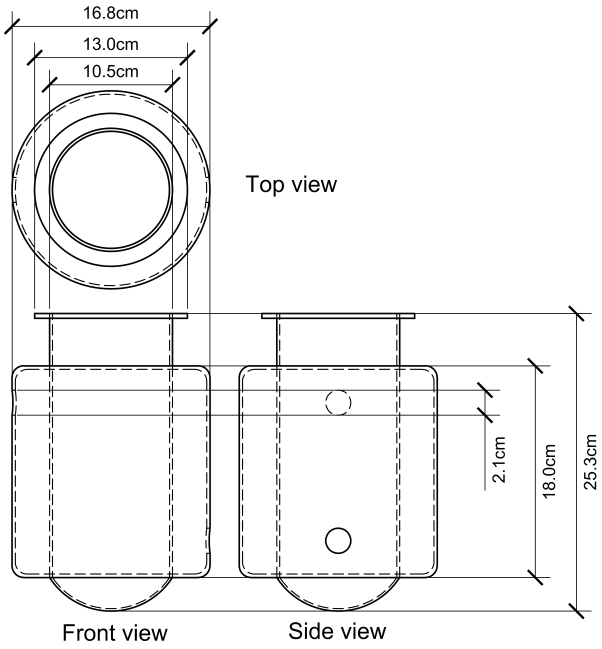


Figure 14. Different views of the reactor designed.

The reactors were equipped with pressure, temperature, and pH sensors for continuous monitoring. The cap was designed to ensure a hermetic system and prevent gas leaks. An expanded view of the reactor and its accessories is shown in Figure 15.

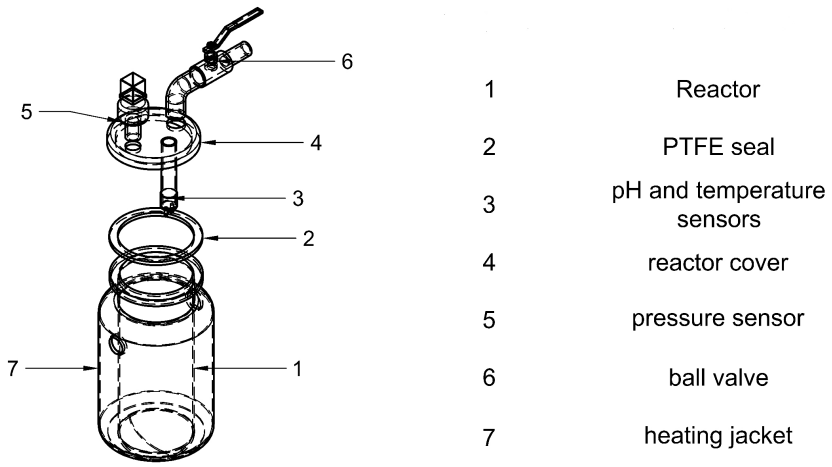


Figure 15. Exploded view of the reactor.

The heat exchange system was simulated under transient conditions by solving Equations (9) and (10), using the parameters listed in Table 5. The simulation was performed over a time range of 0 to 360 s, with an initial temperature of 30.9 °C.

Figure 16 shows the results from solving Equation (9), where the theoretical data obtained from the energy balance is represented by a continuous line, and the experimental data is shown as dots.

Table 5. Thermodynamic and geometric parameters.

Parameter	Value	Units
M	0.08325	kmol
W	0.037	kmol/s
C_{pC}	$72.43 + 0.01039 \cdot T_C + 1.4965 \times 10^{-5} \cdot T_C^2$	kJ/kmol·K
C_{pH}	$72.43 + 0.01039 \cdot T_H + 1.4965 \times 10^{-5} \cdot T_H^2$	kJ/kmol·K
A	0.0613	m^2
U	0.5	kJ/m^2·K

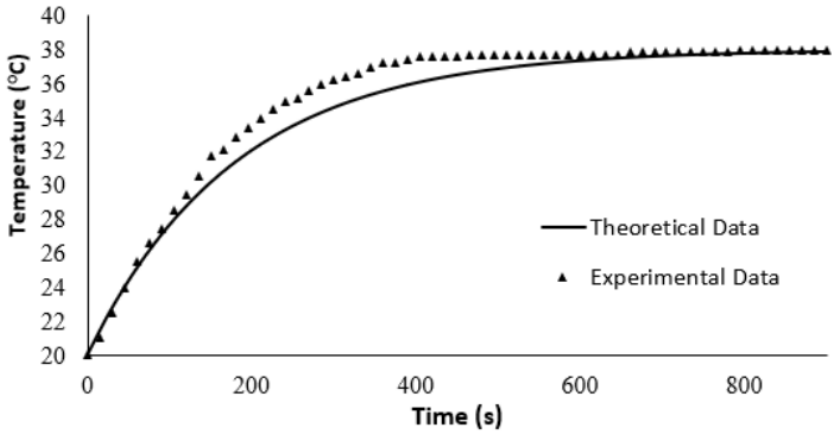


Figure 16. Thermal model validation in the heat exchanger jacket.

The substrate characterization showed a TS of 1.61% and VS of 0.62%, while the inoculum had a TS of 5.78% and VS of 2.08%. Figure 17 presents the pH variation, where an initial drop was observed, attributed to the acidogenic phase of anaerobic digestion [40]. To maintain the pH above 6, NaOH 1 M was added at approximately 5000, 10,000, and 15,000 min. For the remaining duration, pH stabilized between 6 and 7. In this case, the pH result was not neutral or slightly alkaline at the end, it may indicate that the digestion process was not fully balanced. This could happen if the microorganisms were unable to completely convert the intermediate products into methane, leaving residual compounds that affect the pH.

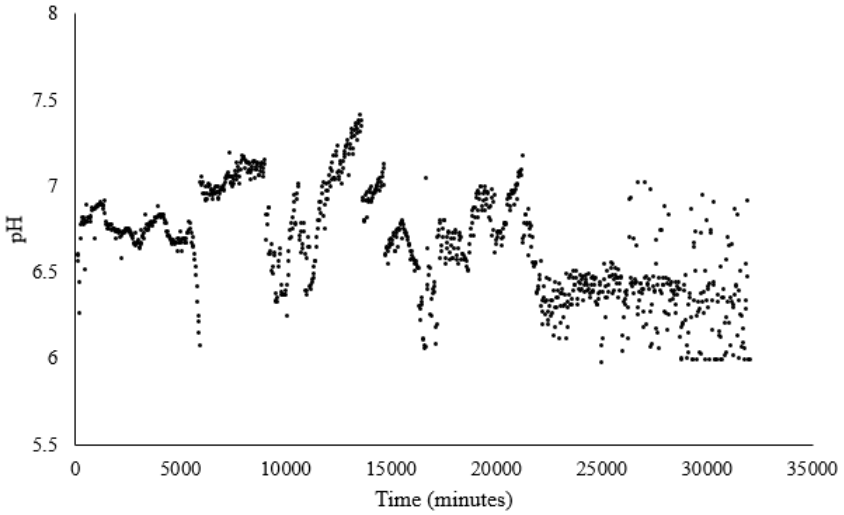


Figure 17. Acquisition data of pH during the BMP test of pig manure.

4. Discussion

The prototype enables continuous pH monitoring, allowing correlation with daily or cumulative methane production and helping to prevent undesirable pH deviations during the test. Temperature, another critical parameter, was also continuously monitored and controlled, with a set-point of 37 °C. As shown in Figure 18, the temperature fluctuated between 35 °C and 40 °C due to the use of an on/off control programmed in PLC1. Although this method can introduce greater variation compared to PID control, it reduces mechanical stress on the pump, the system's main actuator. According to the data logged in the PLC, the pump was activated 96 times over the 22-day test.

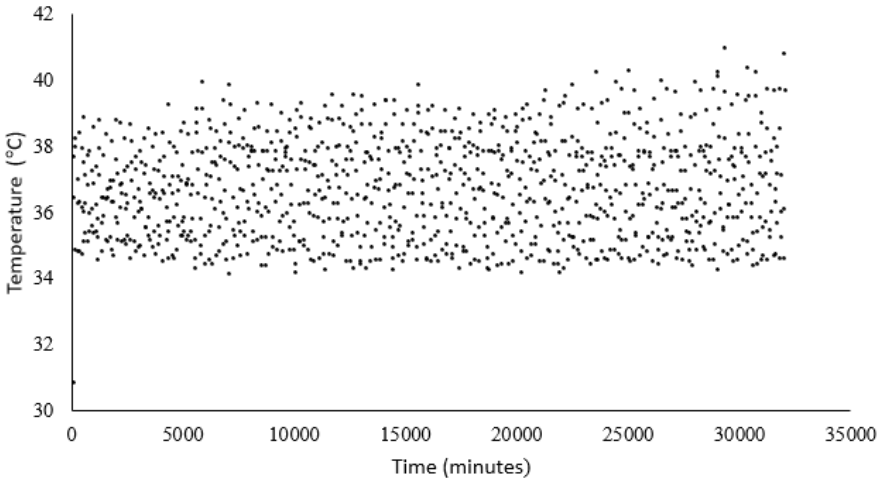


Figure 18. Data acquisition of temperature during the BMP test of pig manure.

The biogas production was measured continuously using two methods. The first one was an indirect method, calculated through the reactor pressure. This pressure can be transformed to standard volume using the combined gases law. The values of biogas were corrected to standard temperature and pressure (STP) conditions (25 °C and 100 kPa). The second one was a direct method. The level sensor shown in Figure 19, which uses the 'tipping bucket' principle, was used. The liquid is displaced by the biogas in a specially designed chamber. The accumulated biogas production is shown for each reactor in Figure 19. A similar behaviour of accumulated methane production in the three reactors can be observed. However, after 25,000 min, when the production start to decrease, the three tests show little difference.

Figure 20a presents the average daily accumulated methane production with a 95% confidence interval, while Figure 20b shows the daily accumulated methane production for each reactor. The average methane production during the test was 493.49 LCH_4, with a specific production of 447.16 LCH_4/kgVS and a standard deviation of 86.23 LCH_4/kgVS. Compared to the 558 LCH_4/kg VS reported by Hidalgo et al. for a similar substrate [5], there is no statistically significant difference at a 5% significance level.

A study carried out in Colombia on pig manure reported values close to 437 LCH_4/kg VS, almost identical to those obtained with the prototype. This evidence shows that the results are not only statistically robust but also comparable with other studies [41]. Likewise, another study reported ranges of 0.29–0.53 m^3 CH_4/kg VS depending on biomass type and experimental conditions, which further supports the similarity of the study's results [42]. We agree that a broader validation against commercial BMP equipment, including multiple substrates, would further strengthen confidence in the system's performance. In this study, however, validation was carried out for a specific substrate as a first step, which was consider relevant for demonstrating the functionality of the prototype.

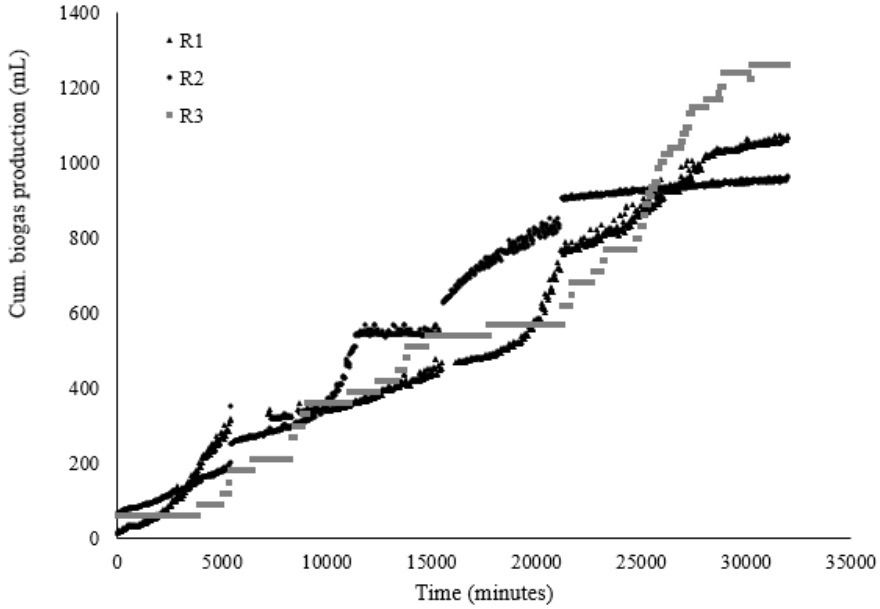
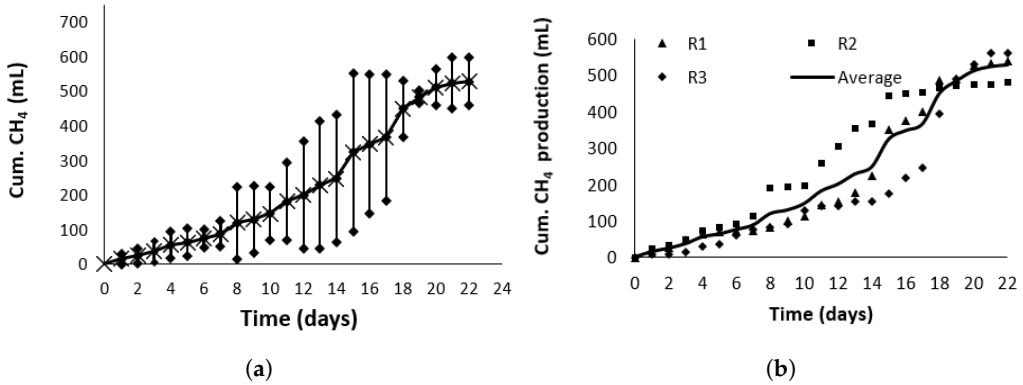


Figure 19. Measure of biogas accumulated in the reactors, R1 and R2 by pressure, R3 by volume.

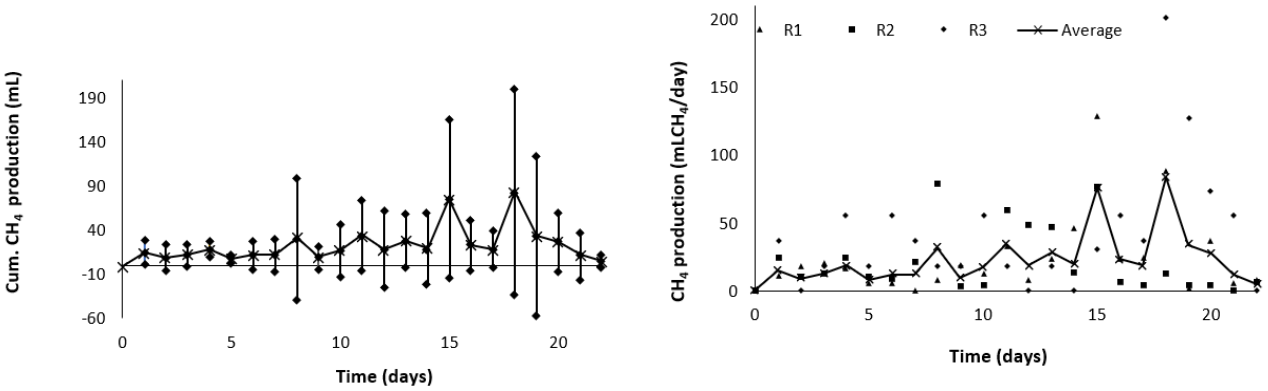


(**a**) (**b**)

Figure 20. (**a**) Confidence interval of daily accumulated methane. (**b**) Accumulated methane production in each reactor.

Figure 21a shows the average daily methane production with a 95% confidence interval, while Figure 21b presents the daily methane production for each reactor. A production peak is observed around day 15, followed by a decline attributed to a reduction in methane concentration—from 74% (v/v) on day 15 to 55% (v/v) by day 20. This drop may result from a decrease in methanogenic bacteria due to substrate depletion [43]. This trend was used as the criterion to conclude the test, indicating that the peak methane production had been surpassed.

The comparison between the prototype and commercial systems is not straightforward, as it largely depends on the specific operating conditions and, above all, on the characteristics of the biomass being tested. In general terms, however, the prototype shows a more limited scope of use compared to the selected alternatives, mainly due to its simpler system for gas collection, storage and data analysis. Furthermore, while the commercial systems employ sensors specifically designed to ensure high-quality operation under standardized conditions, the prototype relies on more basic and accessible sensors that, although functional, are not necessarily specialized for biogas applications.



(**a**) (**b**)

Figure 21. (**a**) Confidence interval of daily methane production. (**b**) Daily methane production in each reactor.

In Table 6 [44–47] some differentiating points can be identified regarding the scope of the commercial products compared.

Table 6. Comparison of key points between the prototype and other commercial products for performing BMP analysis.

Feature	Prototype	AMPTS® III (Bioprocess Control)	RESPIROMETRIC Sensor System 6 Maxi–Velp
Number of reactors	3 (2 L each one)	18 reactors standard, 9 in Light version	6 equipped with sensors
Temperature control precision	Experimental results show that temperature varies ±2 °C	±0.2 °C precision reported for AMPTS III	±1 °C or ±0.5 °C (at 20 °C) in Velp systems
Pressure/Measurement range	The pressure sensors were calibrated over a "global range" of 0 to 15 psig	The equipment is not designed to work with high pressures, it can operate under pressure variations of −0.5 to 0.5 mbar	Pressure range 500–2000 mbar (hPa)
User-interface/data acquisition	Simple data collection system	Aurora™ is the software with functions such as starting and stopping all channels, zooming on graphs, flexible gas normalization, phased agitation control, and raw data download	Velp has proprietary software (RESPIROSoft™), real-time curve display and wireless DataBox
Mixing/stirring	No mixing	AMPTS III includes mechanical agitation	Velp Maxi: uses bottles and may include stirring station

In substrates that are dilute and already well dispersed, mechanical mixing may provide little additional benefit. Rojas et al. [48] reported that in highly diluted media, the contact between bacteria and substrate was sufficient without mixing, achieving similar yields to agitated systems as long as the inoculum was active and capable.

Although literature indicates that agitation can be omitted in systems with dissolved or well-dispersed biomass, it would still be ideal to compare biogas production with and without mixing in the prototype. This comparison would provide a clearer understanding of the process dynamics and confirm whether the absence of agitation affects performance under the specific operating conditions of the system.

5. Conclusions

The prototype developed enables the standardization of the BMP test for easily biodegradable substrates by ensuring homogeneity in operation through its design, configuration, and layout. It maintains stable critical variables such as temperature (automated) and pH (manual), thanks to a real-time electronic data acquisition and control system. Reactor sizing followed heuristic criteria, resulting in a total volume of 2 L, and construction was achieved using SCH 40 stainless steel commercial pipe sections. The heat exchanger design accurately matched expected behavior, with a standard deviation of 1.8—acceptable for this type of test.

The use of open-source and prototyped electronic devices proved effective for monitoring anaerobic digestion. Sensors for pH and temperature ensured process stability, while pressure and flow sensors enabled biogas quantification. A major advantage is continuous data availability, which facilitates later analysis and opens the possibility for remote monitoring via IoT tools, allowing future scale-up.

During the BMP test, variations in pH (6–7) and temperature (35–40 °C) were monitored in real-time. The system's temperature control, managed by an Arduino-Raspberry Pi set-up, demonstrated energy efficiency, with only 96 pump activations over 22 days. Biogas production measured both directly (displaced volume) and indirectly (pressure) showed no statistical differences, validating both methods.

Author Contributions: Conceptualization, O.V.-E. and S.A.-O.; methodology, S.A.-O.; software, S.A.-O. and C.A.Z.-T.; validation, S.A.-O.; formal analysis, S.A.-O.; investigation, S.A.-O. and O.V.-E.; resources, S.A.-O.; writing—original draft preparation, S.A.-O.; writing-review and editing, O.V.-E., S.A.-O. and A.A.-C.; visualization, A.A.-C. and I.A.I.-M.; supervision, I.A.I.-M.; project administration, O.V.-E. and I.A.I.-M.; funding acquisition, O.V.-E. and I.A.I.-M. All authors have read and agreed to the published version of the manuscript.

Funding: This research received no external funding.

Institutional Review Board Statement: Not applicable.

Informed Consent Statement: Not applicable.

Data Availability Statement: Data can be viewed at: https://doi.org/10.5281/zenodo.16911269.

Acknowledgments: The authors acknowledge the support provided by Universidad Pontificia Bolivariana. The authors have reviewed and edited the output and take full responsibility for the content of this publication.

Conflicts of Interest: The authors declare no conflicts of interest.

Abbreviations

The following abbreviations are used in this manuscript:

A	Heat exchanger area (m^2)
$AC1$	Actuator/contactor on-off for the heating system at 220V AC
$AC2$	Actuator/contactor on-off for the pump at 110V AC
C_{pC}	Specific heat capacity of the fluid to be heated (kJ/kmol · K)
C_{pH}	Specific heat capacity of hot water (kJ/kmol · K)
ρ	Water density (kg/m^3)
D_i	Internal diameter of the pipes (m)
D_R	Reactor diameter (m)
ε	Roughness factor of the pipes (m)
f	Friction factor
FT	Gas-flow transmitter
GV	Globe valve

$-K1$	Contactor to pump control
$-K1$	Contactor to thermal resistance control
K_L	Loss coefficient in accessories
L	Length of pipes (m)
$(L/D)_R$	Height-diameter ratio, recommended value is 3 (–)
L_R	Reactor height (m)
LS	Level indicator
M	Moles of the fluid used in the reactor (kmol)
$-M$	Motor Pump
P	Pressure (psig)
$P1$	Pump for recirculation
pH	pH value
pHT	pH transmitter
$PLC1$	Programmable logic controller Arduino-Raspberry
$PLC2$	Programmable logic controller Temperature control
PT	Pressure transmitter
$-Q1$	Thermal magnetic circuit breaker 3 lines
$R_{1,2,3}$	Reactors 1, 2 and 3
$S1$	Pressure sensor-transmitter
$S2$	Pressure sensor-transmitter
$S3$	Pressure sensor-transmitter
$S4$	pH transmitter
$S5$	Temperature transmitter
$S6$	Temperature transmitter
$S7$	Temperature transmitter
$S8$	Level Switch Sensor
SSR	Solid state relay
SV	Screw valve
t	Time (s)
T_H	Temperature of the fluid used in the heat exchanger (K)
T_i	Temperature inside the reactor (K)
TK	Tank for recycling hot-water
TR	Thermal resistance
TS	Temperature indicator
TT	Temperature transmitter
U	Overall coefficient of heat transfer (kJ/m^2 · K)
μ	Water viscosity (kg/m-s)
V	Reactor volume (m^3)
v	Average velocity (m/s)
$\dot{v}$	Volumetric flow (m^3/s)
Vf_R	Free-volume fraction of the reactor, this value is 0.2 (–)
V_1	Signal emitted by the pressure transmitter in bits
$-V1$	5 VDC source
$-V2$	24 VDC source
W	Molar flow of heat fluid used in the heat exchanger (kmol/s)
Z_1	Elevation of the point where the pump takes the hot fluid to heat the reactors (m)
Z_2	Elevation of the point where the pump discharges the fluid after heating the reactors (m)
BMP	Biochemical Methane Potential
AD	Anaerobic Digestion
SV	Solenoid Valve
SCH	Schedule
$VDLUFA$	Verband Deutscher Landwirtschaftlicher Untersuchungs- und Forschungsanstalten
VDI	Verein Deutscher Ingenieure
$IRENA$	Institute of Environment, Natural Resources and Biodiversity
UL	Universidad de León

UPB	Universidad Pontificia Bolivariana
PID	Piping and Instrumentation Diagram
MS	Microsoft
CAPEX	Capital Expenditure
*RKF*45	Runge-Kutta 45
PLC	Programmable Logic Controller
VDC	Direct Current Volts
RTD	Resistance Temperature Detector
*RBP*3	Raspberry Pi 3 Model B®
*AM*2560	Arduino Mega 2560®
IDE	Integrated Development Environment
TS	Total Solids
VS	Volatile Solids
LCH_4	Liters of Methane
WWTP	Wastewater Treatment Plant
APHA	American Public Health Association
VFA	Volatile Fatty Acids
PTFE	Polytetrafluoroethylene
TXD	Transmit Data
RXD	Receive Data

References

1. Cruz, I.A.; de Melo, L.; Leite, A.N.; Melquiades Sátiro, J.V.; Santos Andrade, L.R.; Torres, N.H.; Cabrera Padilla, R.Y.; Bharagava, R.N.; Tavares, R.F.; Romanholo Ferreira, L.F. A new approach using an open-source low cost system for monitoring and controlling biogas production from dairy wastewater. *J. Clean. Prod.* **2019**, *241*, 118284. [CrossRef]
2. Pramanik, S.K.; Suja, F.B.; Zain, S.M.; Pramanik, B.K. The anaerobic digestion process of biogas production from food waste: Prospects and constraints. *Bioresour. Technol. Rep.* **2019**, *8*, 100310. [CrossRef]
3. González, J.; Sánchez, M.E.; Gómez, X. Enhancing Anaerobic Digestion: The Effect of Carbon Conductive Materials. *C* **2018**, *4*, 59. [CrossRef]
4. Zhou, Y.; Xu, Z.; Zhao, M.; Shi, W.; Huang, Z.; He, D.; Ruan, W. Construction and evaluation of efficient solid-state anaerobic digestion system via vinegar residue. *Int. Biodeterior. Biodegrad.* **2018**, *133*, 142–150. [CrossRef]
5. Hidalgo, D.; Martín-Marroquín, J.M. Biochemical methane potential of livestock and agri-food waste streams in the Castilla y León Region (Spain). *Food Res. Int.* **2015**, *73*, 226–233. [CrossRef]
6. Arango-Osorio, S.; Vasco-Echeverri, O.; López-Jiménez, G.; González-Sanchez, J.; Isaac-Millán, I. Methodology for the design and economic assessment of anaerobic digestion plants to produce energy and biofertilizer from livestock waste. *Sci. Total. Environ.* **2019**, *685*, 1169–1180. [CrossRef]
7. Wang, B.; Nges, I.A.; Nistor, M.; Liu, J. Determination of methane yield of cellulose using different experimental setups. *Water Sci. Technol.* **2014**, *70*, 599–604. [CrossRef] [PubMed]
8. Angelidaki, I.; Alves, M.; Bolzonella, D.; Borzacconi, L.; Campos, J.L.; Guwy, A.J.; Kalyuzhnyi, S.; Jenicek, P.; van Lier, J.B. Defining the biomethane potential (BMP) of solid organic wastes and energy crops: A proposed protocol for batch assays. *Water Sci. Technol.* **2009**, *59*, 927–934. [CrossRef]
9. Koch, K.; Bajón Fernández, Y.; Drewes, J.E. Influence of headspace flushing on methane production in Biochemical Methane Potential (BMP) tests. *Bioresour. Technol.* **2015**, *186*, 173–178. [CrossRef]
10. Elbeshbishy, E.; Nakhla, G.; Hafez, H. Biochemical methane potential (BMP) of food waste and primary sludge: Influence of inoculum pre-incubation and inoculum source. *Bioresour. Technol.* **2012**, *110*, 18–25. [CrossRef] [PubMed]
11. Kleinheinz, G.; Hernandez, J. Comparison of two laboratory methods for the determination of biomethane potential of organic feedstocks. *J. Microbiol. Methods* **2016**, *130*, 54–60. [CrossRef]
12. Parthiba Karthikeyan, O.; Trably, E.; Mehariya, S.; Bernet, N.; Wong, J.W.; Carrere, H. Pretreatment of food waste for methane and hydrogen recovery: A review. *Bioresour. Technol.* **2018**, *249*, 1025–1039. [CrossRef]
13. Godin, B.; Mayer, F.; Agneessens, R.; Gerin, P.; Dardenne, P.; Delfosse, P.; Delcarte, J. Biochemical methane potential prediction of plant biomasses: Comparing chemical composition versus near infrared methods and linear versus non-linear models. *Bioresour. Technol.* **2015**, *175*, 382–390. [CrossRef]
14. Rodrigues, R.; Rodrigues, D.; Klepacz-Smolka, A.; Martins, R.; Quina, M. Comparative analysis of methods and models for predicting biochemical methane potential of various organic substrates. *Sci. Total. Environ.* **2019**, *649*, 1599–1608. [CrossRef]

15. Pham, C.H.; Triolo, J.M.; Cu, T.T.T.; Pedersen, L.; Sommer, S.G. Validation and Recommendation of Methods to Measure Biogas Production Potential of Animal Manure. *Asian-Australas. J. Anim. Sci.* **2013**, *26*, 864–873. [CrossRef]
16. Buitrón, G.; Hernández-Juárez, A.; Hernández-Ramírez, M.D.; Sánchez, A. Biochemical methane potential from lignocellulosic wastes hydrothermally pretreated. *Ind. Crop. Prod.* **2019**, *139*, 111555. [CrossRef]
17. Koch, K.; Lippert, T.; Drewes, J.E. The role of inoculum's origin on the methane yield of different substrates in biochemical methane potential (BMP) tests. *Bioresour. Technol.* **2017**, *243*, 457–463. [CrossRef]
18. Holliger, C.; Alves, M.; Andrade, D.; Angelidaki, I.; Astals, S.; Baier, U.; Bougrier, C.; Buffière, P.; Carballa, M.; de Wilde, V.; et al. Towards a standardization of biomethane potential tests. *Water Sci. Technol.* **2016**, *74*, 2515–2522. [CrossRef]
19. Hafner, S.D.; Fruteau de Laclos, H.; Koch, K.; Holliger, C. Improving Inter-Laboratory Reproducibility in Measurement of Biochemical Methane Potential (BMP). *Water* **2020**, *12*, 1752. [CrossRef]
20. Hülsemann, B.; Zhou, L.; Merkle, W.; Hassa, J.; Müller, J.; Oechsner, H. Biomethane Potential Test: Influence of Inoculum and the Digestion System. *Appl. Sci.* **2020**, *10*, 2589. [CrossRef]
21. Owen, W.F.; Stuckey, D.C.; Healy, J.B.; Young, L.; McCarty, P. Bioassay for monitoring biochemical methane potential and anaerobic toxicity. *Water Res.* **1979**, *13*, 485–492. [CrossRef]
22. Gutiérrez-Pulido, H.; De la Vara-Salazar, R. *Análisis y Diseño de Experimentos*, 2nd ed.; McGraw Hill S.A.: Mexico, México, 2008; Volume 736.
23. Wang, B.; Björn, A.; Strömberg, S.; Nges, I.A.; Nistor, M.; Liu, J. Evaluating the influences of mixing strategies on the Biochemical Methane Potential test. *J. Environ. Manag.* **2017**, *185*, 54–59. [CrossRef]
24. Çengel, A.Y.; Cimbala, J.M. *Fluid Mechanics Fundamentals and Applications*, 4th ed.; McGraw Hill S.A.: New York, NY, USA, 2018.
25. Filer, J.; Ding, H.H.; Chang, S. Biochemical Methane Potential (BMP) Assay Method for Anaerobic Digestion Research. *Water* **2019**, *11*, 921. [CrossRef]
26. Çengel, Y.A.; Ghajar, A.J. *Transferencia de Calor y Masa, Fundamentos y Aplicaciones*, 4th ed.; McGraw Hill S.A.: Mexico, México, 2011.
27. Kern, D.Q. *Procesos de Transferencia de Calor*; 1965 ed.; McGraw Hill S.A.: Mexico, México, 1999.
28. Burton, M. Arduino Temperature Control Library. GitHub Library. 2020. Available online: https://github.com/milesburton/Arduino-Temperature-Control-Library (accessed on 21 October 2025).
29. Stroffregen, P. Library for Dallas/Maxim 1-Wire Chips. GitHub Library. 2017. Available online: https://github.com/PaulStoffregen/OneWire (accessed on 21 October 2025).
30. Devore, J.L. *Probabilidad y Estadística para Ingeniería y Ciencias*, 7th ed.; Cengage: Mexico, México, 2008.
31. DFROBOT. Measure pH efficiently with a low-cost sensor for Arduino. Offers ±0.1 accuracy, easy connection, ideal for water quality testing and aquaponics projects. Gravity: Lab Grade Analog pH Sensor Kit for Arduino. Available online: https://www.dfrobot.com/product-1025.html (accessed on 21 October 2025).
32. Wu, Z.L.; Lin, Z.; Sun, Z.Y.; Gou, M.; Xia, Z.Y.; Tang, Y.Q. A comparative study of mesophilic and thermophilic anaerobic digestion of municipal sludge with high-solids content: Reactor performance and microbial community. *Bioresour. Technol.* **2020**, *302*, 122851. [CrossRef]
33. Amodeo, C.; Hafner, S.D.; Teixeira Franco, R.; Benbelkacem, H.; Moretti, P.; Bayard, R.; Buffière, P. How Different Are Manometric, Gravimetric, and Automated Volumetric BMP Results? *Water* **2020**, *12*, 1839. [CrossRef]
34. Nayyar, A.; Puri, V. Raspberry Pi-A Small, Powerful, Cost Effective and Efficient Form Factor Computer: A Review. *Int. J. Adv. Res. Comput. Sci. Softw. Eng.* **2015**, *5*, 720–737.
35. Arduino. Open-Source Electronic Prototyping Platform Enabling Users to Create Interactive Electronic Objects. Empowering Anyone to Innovate. Available online: https://www.arduino.cc/ (accessed on 21 October 2025).
36. APHA. *Standard Methods For the Examination of Water and Wastewater*; APHA: Washington, DC, USA, 2005.
37. Alexis, P.O.B.; Patricia, T.L.; Fernando, M.R.L.; Marcela, C.C.L.; Carlos, V.F.; Alexander, T.L.W.; Abdón, O.A.J. Efecto de la relación sustrato-inóculo sobre el potencial bioquímico de metano de biorresiduos de origen municipal. *Ing. Investig. Tecnol.* **2015**, *16*, 515–526. [CrossRef]
38. Perry, R.H.; Green, D.W. *Perry's Chemical Engineer's Handbook*, 7th ed.; McGraw Hill S.A.: New York, NY, USA, 1997.
39. Pearse, L.F.; Hettiaratchi, J.P.; Kumar, S. Towards developing a representative biochemical methane potential (BMP) assay for landfilled municipal solid waste—A review. *Bioresour. Technol.* **2018**, *254*, 312–324. [CrossRef]
40. Kafle, G.K.; Chen, L. Comparison on batch anaerobic digestion of five different livestock manures and prediction of biochemical methane potential (BMP) using different statistical models. *Waste Manag.* **2016**, *48*, 492–502. [CrossRef]
41. Rodríguez, A.; Ángel, J.; Rivero, E.; Acevedo, P.; Santis, A.; Cabeza, I.; Acosta, M.; Hernández, M. Evaluation of the biochemical methane potential of pig manure, organic fraction of municipal solid waste and cocoa industry residues in Colombia. *Chem. Eng. Trans.* **2017**, *57*, 55–60. [CrossRef]
42. García-de-la Fuente, R.; Cuesta, G.; Sanchís-Jiménez, E.; Botella, S.; Abad, M.; Fornes, F. Bacteria involved in sulfur amendment oxidation and acidification processes of alkaline 'alperujo' compost. *Bioresour. Technol.* **2011**, *102*, 1481–1488. [CrossRef] [PubMed]

43. Romero-Güiza, M.; Vila, J.; Mata-Alvarez, J.; Chimenos, J.; Astals, S. The role of additives on anaerobic digestion: A review. *Renew. Sustain. Energy Rev.* **2016**, *58*, 1486–1499. [CrossRef]
44. BPC Instruments. The Market-Leading Analytical Tool for Anaerobic Batch Fermentation Testing. Available online: https://bpcinstruments.com/wp-content/uploads/2023/03/AMPTS-III-20230317.pdf (accessed on 21 October 2025).
45. Fisher Scientific Velp Scientifica^{TM} RESPIROMETRIC Sensor System 6 Maxi-BMP. Available online: https://www.fishersci.co.uk/shop/products/respirometric-sensor-system-6-maxi-bmp-2/p-7089890 (accessed on 21 October 2025).
46. Fisher Scientific. RESPIROMETRIC Sensor. Available online: https://www.velp.com/public/file/VELPRESPIROMETRIC-SENSORrev02-1-273869.pdf (accessed on 21 October 2025).
47. RESPIROMETRIC Sensor System 6 Maxi. Available online: https://faustlabscience.de/en/RESPIROMETRIC-Sensor-System-6-Maxi/4685936 (accessed on 21 October 2025).
48. Rojas, C.; Fang, S.; Uhlenhut, F.; Borchert, A.; Stein, I.; Schlaak, M. Stirring and biomass starter influences the anaerobic digestion of different substrates for biogas production. *Eng. Life Sci.* **2010**, *10*, 339–347. [CrossRef]

Disclaimer/Publisher's Note: The statements, opinions and data contained in all publications are solely those of the individual author(s) and contributor(s) and not of MDPI and/or the editor(s). MDPI and/or the editor(s) disclaim responsibility for any injury to people or property resulting from any ideas, methods, instructions or products referred to in the content.